Molecular Plant Pathology

MOLECULAR PLANT PATHOLOGY (2018) 19(6), 1353–1363 DOI: 10.1111/mpp.12619

The feruloyl esterase genes are required for full pathogenicity of the apple tree canker pathogen *Valsa mali*

MING XU, XIAONING GAO*, JILIANG CHEN, ZHIYUAN YIN, HAO FENG AND LILI HUANG*

State Key Laboratory of Crop Stress Biology for Arid Areas, College of Plant Protection, Northwest A&F University, Yangling, Shaanxi 712100, China

SUMMARY

Apple Valsa canker, caused by the fungus *Valsa mali*, is one of the most destructive diseases of apple trees in East Asia. Feruloyl esterases (ferulic acid esterases, FAEs), which belong to a subclass of carboxylic esterases, can cleave ester bonds that crosslink hydroxycinnamic acids and arabinoxylans or certain pectins in plant cell walls. However, a pathogenic role of FAE has not been demonstrated in plant-pathogenic fungi. In this study, the *FAE* gene family, including one type A, one type B, three type C and two type D *FAE* genes, was identified in *V. mali*. Five of the seven *FAE* genes had highly elevated transcript levels in *V. mali*–apple tree bark interactions compared with mycelia grown in axenic culture. Signal peptides of the VmFAEs were confirmed using yeast signal sequence trap assays. To examine whether *FAE*s are required for the pathogenicity of *V. mali*, seven single- and six double-gene deletion mutants were generated. Compared with the wild-type, three of the seven *FAE* single-deletion mutants showed significantly reduced pathogenicity and three of the six *FAE* double-deletion mutants exhibited greater reductions in pathogenicity, suggesting the joint action of *FAE*s in the *V. mali*–apple tree interaction. Most of the *FAE* mutants that exhibited a significant reduction in pathogenicity had significantly lower FAE activity than the wild-type fungus. These results indicate that secreted FAEs are required for the full pathogenicity of the phytopathogenic fungus *V. mali*.

Keywords: apple tree Valsa canker, cell wall-degrading enzyme, FAE, pathogenicity, secretion.

INTRODUCTION

Plant cells are surrounded by three-dimensional plant cell walls formed from a tight complex polysaccharide network that consists primarily of cellulose, hemicelluloses, pectin and a small number of structural proteins (Cosgrove, 2005). Plant cell walls are strengthened by ester linkages, which covalently bind hydroxycinnamic acids to polysaccharides (Benoit *et al.*, 2006; Gopalan *et al.*, 2015; Ishii, 1997). Some plant cells are additionally surrounded by a secondary cell wall formed by a thick layer of cellulose associated with lignin. This stable structure of plant cell walls provides effective protection against microorganisms (Dixon, 2013). In parallel, phytopathogens have evolved powerful arsenals to break down plant cell walls. Most plant pathogens secrete a complex mixture of hydrolytic enzymes, which enable the pathogens to penetrate and infect the host (Kubicek *et al.*, 2014). These extracellular hydrolytic enzymes are called cell wall-degrading enzymes (CWDEs) (Guerriero *et al.*, 2015; Kikot *et al.*, 2009; Walton, 1994). CWDEs are essential for phytopathogens that do not have specialized penetration structures (Kikot *et al.*, 2009). In addition, many phytopathogens require CWDEs during the late stages of infection for the killing and degradation of plant tissue to utilize nutrients for growth and reproduction (Kubicek *et al.*, 2014).

Feruloyl esterases (ferulic acid esterases, FAEs) [EC 3.1.1.73] (also known as cinnamic acid hydrolases, cinnamoyl esterases or *p*-coumaroyl esterases) belong to a subclass of carboxylic esterases, which are hemicellulases [EC 3.1.1] (Topakas *et al.*, 2007). FAEs cleave ester bonds that crosslink hydroxycinnamic acids and arabinoxylans or certain pectins in plant cell walls. Four subclasses, termed types A, B, C and D, have been classified based on their sequence characteristics and substrate utilization (Crepin *et al.*, 2004). FAEs have been well characterized for their potential applications in many industries, including the chemical, food, pharmaceutical, cosmetics, fuel, textile, pulp and paper industries (Pinto, 2015). FAEs are thought to play an important role in the complete degradation of plant cell wall polysaccharides and in loosening the cell wall structure by hydrolysing the ferulate ester groups involved in the crosslinks between hemicellulose and lignin (Gopalan *et al.*, 2015; de Vries & Visser, 1999; Wong, 2006), thereby facilitating the access of depolymerases to the cell wall polymer backbones (Hermoso *et al.*, 2004; Kikot *et al.*, 2009).

Apple Valsa canker, caused by *Valsa mali*, is one of the most destructive diseases of apple trees in East Asia (Vasilyeva & Kim, 2000; Wang *et al.*, 2014). *V. mali* exhibits only weak parasitism because this fungus parasitizes mainly through bark wounds and cracks (Adams *et al.*, 2006; Biggs, 1989; Ke *et al.*, 2013; Kepley & Jacobi, 2000). After the infection of wounded tissue, hyphae develop intra- and intercellularly and colonize bark tissue surrounding the penetration sites, which induces severe tissue maceration and necrosis (Ke *et al.*, 2013). The genome and transcriptome of *V. mali* during the infection of apple bark have been

* *Correspondence*: Lili Huang: Email: huanglili@nwsuaf.edu.cn, Xiaoning Gao: Email: gxning@nwsuaf.edu.cn

sequenced. A whole-genome analysis has revealed that the *V. mali* genome encodes a plethora of pathogenicity-related genes involved in plant cell wall degradation and secondary metabolite biosynthesis (Yin *et al.*, 2015). Transcriptome profiling has also suggested that cell wall hydrolases are important for disease establishment (Ke *et al.*, 2014). In our previous study, a transfer DNA (T-DNA) insertion mutant with reduced virulence was identified (Hu *et al.*, 2014; Huang *et al.*, 2014). The insertion was annotated in the *FAEB* gene (Huang *et al.*, 2014). The objective of this study was to provide insights into the potential functions of *FAE* during *V. mali* infection.

RESULTS

Sequence identification, phylogenetic analysis and sequence alignment of *V. mali* FAEs

BLAST searches with the four well-characterized types of *FAE* sequence showed that seven putative *FAE* genes (*VM1G_01793*, *VM09901*, *VM04403*, *VM1G_00022*, *VM1G_06347*, *VM1G_06527* and *VM1G_00901*) were encoded by the genome of *V. mali*. All seven *FAE* genes were amplified by polymerase chain reaction (PCR) from a cDNA library of *V. mali* and confirmed by sequencing. The conserved domains of the candidate *FAE* genes were showed in Fig. S1.

To determine the type and to understand the evolutionary relationship of the predicted *V. mali* FAEs, the protein sequences of these predicted proteins and those of certain characterized FAEs and some related CWDEs were aligned using CLUSTALW, and the alignment result was used to build a neighbour-joining phylogenetic tree (Fig. 1A). The phylogenetic tree indicates that FAEs from *V. mali* can be divided into four subgroups, types A, B, C and D, according to the classification standard of Crepin *et al.* (2004). The phylogenetic tree shows that one type A, one type B, three type C and two type D *FAE*s are encoded by the genome of *V. mali* (Fig. 1A). Therefore, the genes *VM1G_01793*, *VM09901*, *VM04403*, *VM1G_00022*, *VM1G_06347*, *VM1G_06527* and *VM1G_00901* were named *VmFAEA1*, *VmFAEB1*, *VmFAEC1*, *VmFAEC2*, *VmFAEC3*, *VmFAED1* and *VmFAED2*, respectively. Notably, fungal lipases (*Thermomyces lanuginosus* lipase AAC08588 and *Neurospora crassa* lipase CAC28687) have high sequence identity with the type A FAEs, which has been shown in a previous study (Crepin *et al.*, 2004). VmFAEB1 is closely related to FgFAEB3 (XP_011325310) from *Fusarium graminearum*. The three VmFAECs are closely related to the FAECs from *F. graminearum*. The two VmFAEDs have a close evolutionary relationship with FAEs from *Diaporthe ampelina* and *Grosmannia clavigera*.

All five type A FAEs and the two lipase sequences aligned using the CLUSTALW program have a common motif (GHSLG) (Fig. 1B). The alignment of the type B FAEs revealed a GXSLG motif, where X stands for S, T, D or V (Fig. 1B). The alignment of the type C FAEs showed a GX_1SX_2GG motif, where X_1 stands for C or G and X_2 is L or T (Fig. 1B). The alignment of the type D FAEs also revealed a GX_1SX_2GG motif, but X_1 stands for F, W or K and X_2 is Q, Y or N (Fig. 1B). In contrast with the former findings, both type C and type D FAEs have the 'GX_1SX_2GG' rather than the 'GX_1SX_2G' motif (Fig. 1B). The conserved motif of these seven predicted *V. mali* FAEs presumably indicates that they are FAEs.

Five *FAE* genes are highly up-regulated during *V. mali* infection of apple bark tissue

To examine the transcript level of *FAE* genes during the interaction of *V. mali* with apple tree bark and in mycelia grown in axenic culture, we sampled infected apple bark tissue at 3 days post-inoculation (dpi) and compared transcript levels with those of mycelia grown in axenic culture for 3 days. The quantitative reverse transcription-polymerase chain reaction (qRT-PCR) assays showed that the *FAE* genes (*VmFAEA1*, *VmFAEB1*, *VmFAEC1*, *VmFAEC2* and *VmFAED1*) were up-regulated on interaction of *V. mali* with apple tree bark (Fig. 2). *VmFAEA1* was the most up-regulated gene with a nearly 15-fold increase in the transcript level. *VmFAEB1* was up-regulated nearly six-fold. The two type C *FAE* genes, *VmFAEC1* and *VmFAEC2*, were up-regulated more than 11- and nine-fold, respectively. The *VmFAED1* gene was up-regulated nearly five-fold. Overall, the high induction of *FAE* genes during infection suggests a potential role in the pathogenicity of *V. mali*.

Valsa mali FAEs possess signal peptides (SPs)

To verify whether the FAEs of *V. mali* are secreted, amino acid sequences were analysed using the SignalP 4.1 Server (http://www.cbs.dtu.dk/services/SignalP/) (Petersen *et al.*, 2011). The results suggest that all the FAEs of *V. mali* contain SPs (Fig. S2, see Supporting Information). To experimentally validate this prediction, the SP-encoding sequences of five *V. mali* FAEs were successfully cloned into the pSUC2 vector (Jacobs *et al.*, 1997). Like the positive control Avr1b, the transformants containing pSUC2-VmFAE-SP could grow in both CMD-W medium (yeast growth without invertase secretion) and YPRAA medium (growth only when invertase is secreted) (Fig. 3). However, transformants with negative control pSUC2-Mg87 or empty vector pSUC2 could not grow in YPRAA (Fig. 3). These results indicate that *V. mali* FAEs contain SPs. The bioinformatics predictions, together with the experimental verification, suggest that the FAEs of *V. mali* are secreted.

Generation of *FAE* gene deletion mutants and complementation transformants

To verify the function of *FAE*s in *V. mali*, single-deletion mutants of all seven *FAE* genes were generated (Table 1). The mutants were examined via PCR assays (Fig. S4, see Supporting Information) and Southern blot analysis (Fig. S5, see Supporting Information). When probed with hygromycin B phosphotransferase gene (*HPH*) or neomycin resistance gene (*NEO*) fragments, the

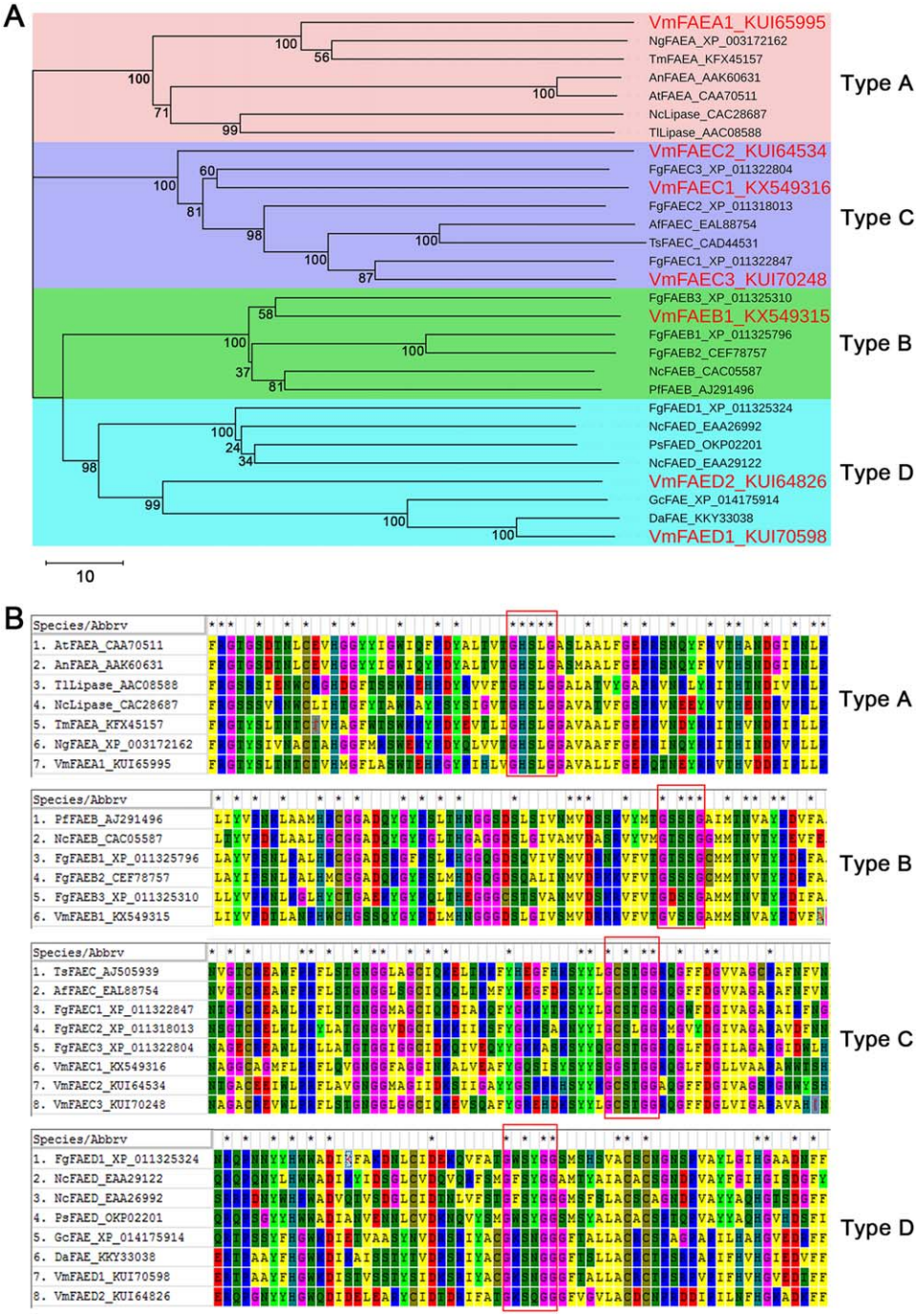

Fig. 1 Phylogenetic tree of ferulic acid esterases (FAEs) and alignment of different types of FAE. (A) Phylogenetic tree of the FAEs. A neighbour-joining phylogenetic tree was constructed using MEGA7. Bootstrap values were set to 1000 repetitions. NgFAEA_XP_003172162, *Nannizzia gypsea* FAEA; TmFAEA_KFX45157, *Talaromyces marneffei* FAEA; AnFAEA_AAK60631, *Aspergillus niger* FAEA; AtFAEA_CAA70511, *Aspergillus tubingensis* FAEA; NcLipase_CAC28687, *Neurospora crassa NcFAE* lipase; TlLipase_AAC08588, *Thermomyces lanuginosus* lipase; FgFAEB1_XP_011325796, *Fusarium graminearum* FAEB1; FgFAEB2_CEF78757, *F. graminearum* FAEB2; FgFAEB3_XP_011325310, *F. graminearum* FAEB3; NcFAEB_CAC05587, *N. crassa* FAEB; PfFAEB_AJ291496, *Penicillium funiculosum* FAEB; FgFAEC1_XP_011322847, *F. graminearum* FAEC1; FgFAEC2_XP_011318013, *F. graminearum* FAEC2; FgFAEC3_XP_011322804, *F. graminearum* FAEC3; AfFAEC_EAL88754, *Aspergillus fumigatus* FAEC; TsFAEC_CAD44531, *Talaromyces stipitatus* FAEC; FgFAED1_XP_011325324, *F. graminearum* FAED1; NcFAED_EAA29122, *N. crassa* NcFAED; PsFAED_OKP02201, *Penicillium subrubescens* FAED; NcFAED_EAA26992, *N. crassa* NcFAED; GcFAE_XP_014175914, *Grosmannia clavigera* FAE; DaFAE_KKY33038, *Diaporthe ampelina* FAE. (B) Alignment of the different types of FAE. The alignment results show the conserved motifs of the four types of FAE. The sequence alignment was performed using the CLUSTALW program in MEGA7. Red rectangles indicate conserved motifs of the different types of FAE.

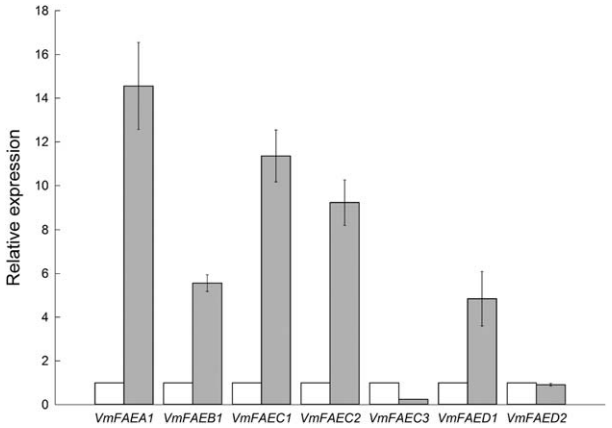

Fig. 2 Transcription levels of the *ferulic acid esterase* (*FAE*) genes in *Valsa mali*. The expression levels of the *VmFAE*s in *in vitro* hyphae were set to unity, represented by white columns. The relative expression of *VmFAE*s (represented by grey columns) during the interaction of *V. mali* with apple bark was normalized by *glucose-6-phosphate dehydrogenase* (*G6PDH*). The means and standard deviations of the transcription levels were calculated from three independent experiments. Bars represent the standard deviations.

wild-type sample showed no hybridization signal. However, a hybridization signal of the expected size was recorded on analysis of the transformants. When hybridized with *FAE* gene probes generated from the PCR products amplified using the gene-specific primers 5F/6R (Table S1, see Supporting Information), the wild-type sample exhibited the expected bands, but the *FAE* mutants lacked a hybridization signal (Fig. S5). To examine whether VmFAEs undergo joint action and redundancy, six types of *FAE* double-deletion mutant were generated and examined via PCR assays or Southern blot analysis (Figs S4 and S5; Table 1).

For the complementation of single *FAE* deletion mutants, a complementary construct was generated and transformed into the corresponding mutant. All the complementation transformants were confirmed by PCR assays (Fig. S6, see Supporting Information). In addition, RT-PCRs were also conducted to confirm that the target *VmFAE* genes were knocked out in the gene deletion mutants and that the complementation strains contained the corresponding target genes (Fig. S7, see Supporting Information).

Deletion of *FAE*s does not affect vegetative growth or pycnidium formation

To investigate whether *FAE*s play a role in the vegetative growth and development of *V. mali*, the growth rate, colony and hyphal morphology, and pycnidium formation of the *FAE* deletion mutants and the wild-type fungus were analysed. No obvious differences in colony morphology or growth rate were observed (Fig. 4). *FAE* deletion mutants can form pycnidia similar to those of the wild-type fungus (Fig. S8A, see Supporting Information). There was also no significant difference between the *FAE* deletion mutants and wild-type samples with regard to the number of pycnidia per square centimetre (Fig. S8B). These results indicate that *FAE* does not affect the vegetative growth or pycnidium formation.

FAE genes contribute to *V. mali* virulence

The elevated transcript levels of *FAE*s during infection and the secretion of FAEs suggest that FAEs may contribute to *V. mali* virulence. The results of the infection assays on twigs of *Malus* × *domestica* Borkh. cv. Fuji showed that the *VmFAEA1*, *VmFAEB1* and *VmFAEC1* deletion mutants were significantly reduced in pathogenicity (with reductions of 12%, 15% and 14%, respectively) compared with the wild-type (Fig. 5A–C). However, the pathogenicity of *VmFAEC2*, *VmFAEC3*, *VmFAED1* and *VmFAED2* deletion mutants was not significantly different from that of the wild-type (Fig. S9A,B,E,F, see Supporting Information). To confirm that the reduced pathogenicity of the mutants was caused by deletion of *VmFAE*, each complementary construct was generated and transformed into the corresponding mutant. The reduced

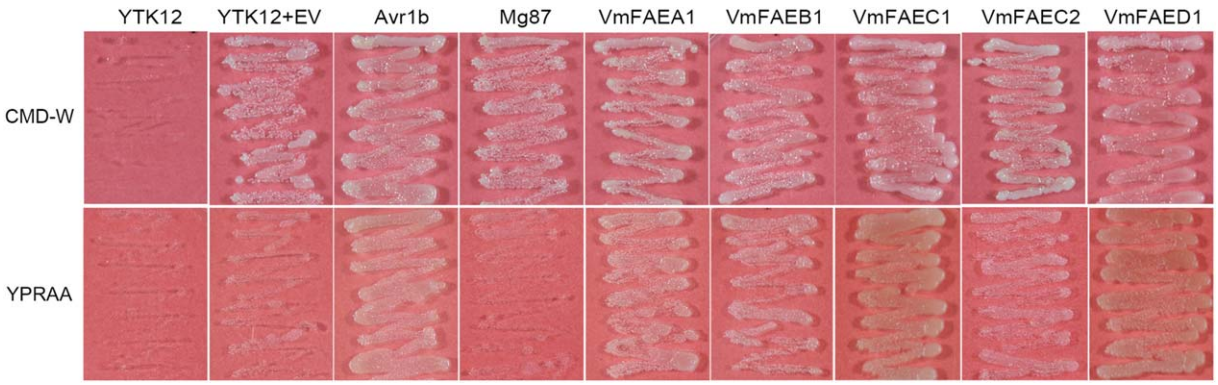

Fig. 3 Functional validation of the signal peptides of *Valsa mali* ferulic acid esterases (FAEs). The coding sequences of the five VmFAE-predicted signal peptides, the signal peptide of Avr1b (positive control) and the first 25 amino acids of Mg87 (negative control) were successfully fused in-frame to the invertase sequence in the pSUC2 vector. YTK12 alone and YTK12 carrying the empty vector pSUC2 (YTK12 + EV) served as additional negative controls.

Table 1 Wild-type and mutant strains of *Valsa mali* used in this study.

Strain	Description
03-8	Wild-type
A1-52	*VmFAEA1* deletion mutant of 03-8
A1-60	*VmFAEA1* deletion mutant of 03-8
B1-5	*VmFAEB1* deletion mutant of 03-8
B1-23	*VmFAEB1* deletion mutant of 03-8
C1-71	*VmFAEC1* deletion mutant of 03-8
C1-116	*VmFAEC1* deletion mutant of 03-8
C2-6	*VmFAEC2* deletion mutant of 03-8
C2-57	*VmFAEC2* deletion mutant of 03-8
C3-24	*VmFAEC3* deletion mutant of 03-8
C3-55	*VmFAEC3* deletion mutant of 03-8
D1-35	*VmFAED1* deletion mutant of 03-8
D1-69	*VmFAED1* deletion mutant of 03-8
D2-14	*VmFAED2* deletion mutant of 03-8
D2-24	*VmFAED2* deletion mutant of 03-8
A1B1-3	*VmFAEB1* deletion mutant of A1-52
A1B1-41	*VmFAEB1* deletion mutant of A1-52
B1C1-15	*VmFAEC1* deletion mutant of B1-5
B1C1-18	*VmFAEC1* deletion mutant of B1-5
C1C2-10	*VmFAEC2* deletion mutant of C1-71
C1C2-35	*VmFAEC2* deletion mutant of C1-71
B1D1-25	*VmFAED1* deletion mutant of B1-5
B1D1-34	*VmFAED1* deletion mutant of B1-5
C1D1-17	*VmFAED1* deletion mutant of C1-71
C1D1-62	*VmFAED1* deletion mutant of C1-71
D1D2-45	*VmFAED2* deletion mutant of D1-35
D1D2-86	*VmFAED2* deletion mutant of D1-35
A1C	*VmFAEA1* complementation transformant of A1-52
B1C	*VmFAEB1* complementation transformant of B1-5
C1C	*VmFAEC1* complementation transformant of C1-71
C2C	*VmFAEC2* complementation transformant of C2-57
D1C	*VmFAED1* complementation transformant of D1-35

pathogenicity was rescued in the complementation strains (Fig. 5A–C). These results suggest that the deletion of these *FAE* genes gives rise directly to the reduction in pathogenicity.

To determine whether the *FAE*s function cooperatively, we inoculated twigs of *M.* × *domestica* Borkh. cv. Fuji with the double-deletion mutants. Although no significant differences were found between the *VmFAEB1C1*, *VmFAEB1D1* and *VmFAED1D2* double-deletion mutants and the wild-type (Fig. S9C,D,G), the *VmFAEA1B1*, *VmFAEC1C2* and *VmFAEC1D1* double-deletion mutants exhibited a significant reduction in lesion size (22%, 28% and 23%, respectively) (Fig. 5D–F). This result indicates that the FAEs may act cooperatively during the *V. mali*–apple tree bark interaction.

FAE deletion mutants exhibit significantly lower FAE activity than that observed in the wild-type fungus

To detect FAE activity, the wild-type fungus and mutants were cultured on MS (Murashige and Skoog) medium containing 0.2% (w/v) ethyl ferulate as the sole carbon source. The MS medium containing 0.2% (w/v) ethyl ferulate was opaque. The utilization of ethyl ferulate by the fungal strain generated clear zones. The cleared zones of the *VmFAEA1*, *VmFAEB1* and *VmFAEC1* deletion mutants and the *VmFAEA1B1* and *VmFAEC1C2* double-deletion mutants were significantly smaller than those of the wild-type fungus (Fig. 6), suggesting that the deletion of *FAE* caused a decrease in FAE activity.

DISCUSSION

The pathogenic role of the CWDEs of phytopathogens has been elucidated by several previous studies (Bravo Ruiz *et al.*, 2016; Feng, 2005; Fu *et al.*, 2013; Van Vu *et al.*, 2012). FAEs are components of hemicellulolytic enzyme systems in microorganisms

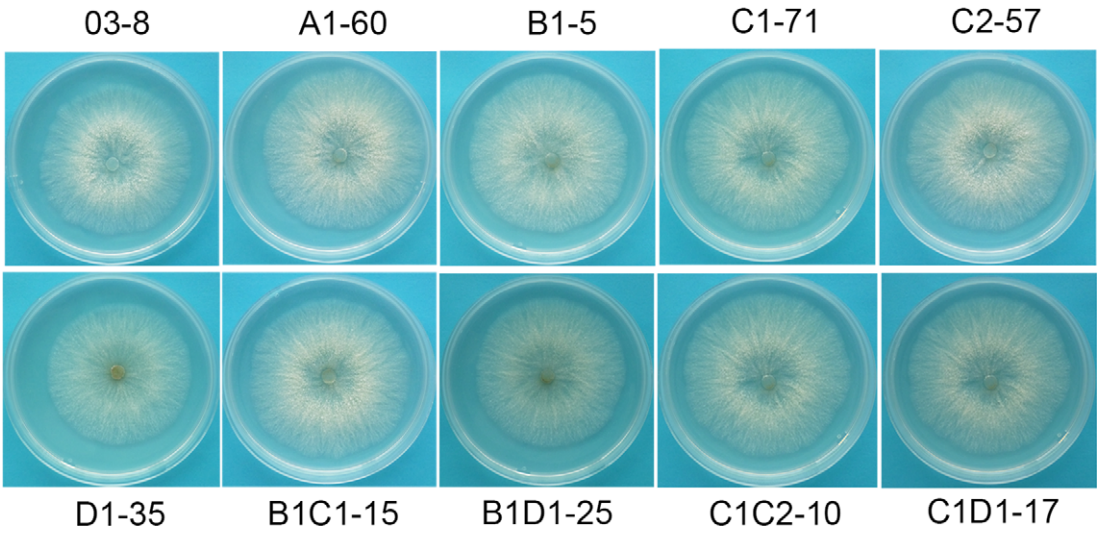

Fig. 4 Colony morphology and colour of wild-type and *ferulic acid esterase* (*FAE*) gene deletion mutants. The wild-type and *FAE* gene deletion mutants were cultured on potato dextrose agar (PDA) at 25°C in the dark. Photographs were taken at 2 days post-culture.

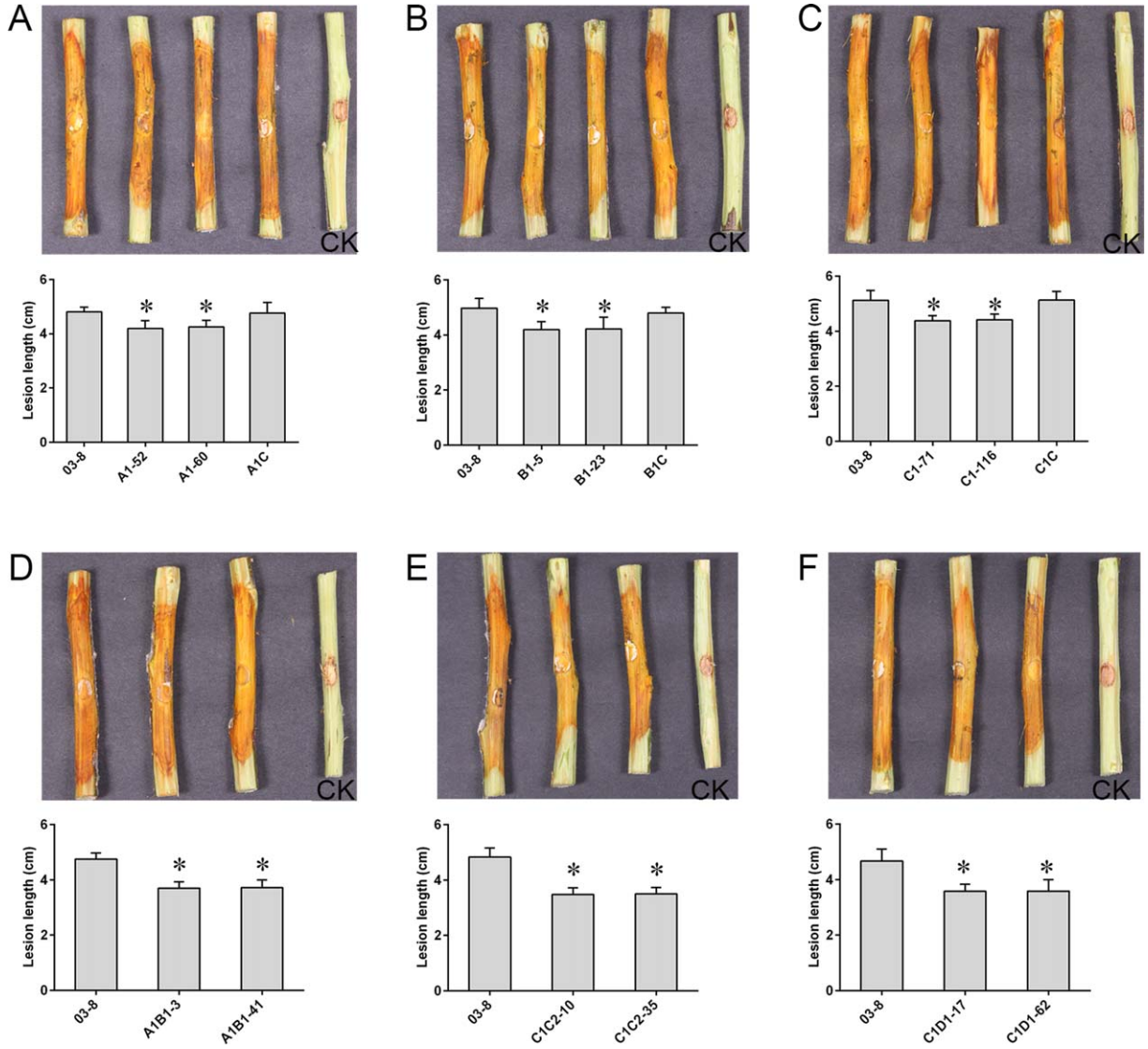

Fig. 5 Pathogenicity assays. The wild-type, *ferulic acid esterase* (*FAE*) gene deletion mutants and complementation strains were inoculated onto twigs of *Malus* × *domestica* Borkh. cv. Fuji. SYA (sucrose–yeast extract–agar) medium plugs ($d = 5$ mm) were used as control (CK). Photographs were taken at 5 days post-inoculation (dpi). The mean lesion length was calculated from three independent pathogenicity experiments with three duplicates per experiment. Bars represent the standard deviation. Asterisks represent statistically significant difference (least-significant difference test, $P < 0.05$). A-F, pathogenicity assays of *VmFAEA1*, *VmFAEB1*, *VmFAEC1* deletion mutants and *VmFAEA1B1*, *VmFAEC1C2*, *VmFAEC1D1* double deletion mutants.

(Topakas *et al.*, 2007). FAEs function at the ester bond between hydroxycinnamic acids and arabinoxylans or certain pectins present in plant cell walls, leading to enhanced accessibility for enzymatic attack on the cell wall polymer backbones. Since the release of ferulic acid from wheat bran involving FAEs was first detected in cultures of *Streptomyces olivochromogenes* (Mackenzie *et al.*, 1987), many FAEs have been identified, purified and partially characterized from fungi or bacteria (Borneman *et al.*, 1992; Faulds & Williamson, 1994; Topakas *et al.*, 2007; Wong *et al.*, 2011). Although microbial FAEs have been widely used for numerous purposes, the roles of FAEs in pathogenesis remain largely unknown. In this study, we have shown that the secreted FAEs are required for the full virulence of *V. mali*.

In a previous study, three type B, three type C and one type D *FAE* gene were identified in *F. graminearum*, and the *FAE* genes showed host-specific gene expression (Balcerzak *et al.*, 2012). In this study, we identified seven *FAE* genes in *V. mali*, including one type A, one type B, three type C and two type D *FAE* genes. Compared with *F. graminearum*, which infects wheat, barley and maize, *V. mali* specifically infects apple trees. The difference in the type and number of *FAE*s probably indicates the diversity of the infection process amongst the different plant-pathogenic fungi.

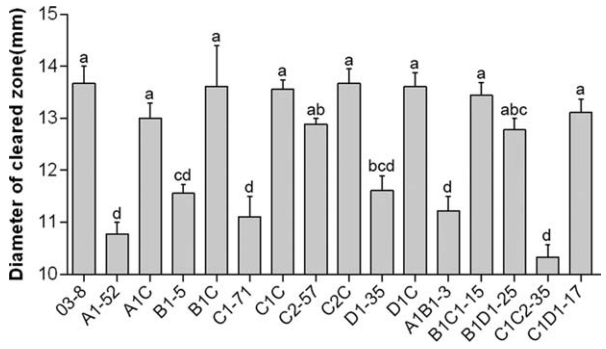

Fig. 6 Detection of ferulic acid esterase (FAE) activity of *FAE* gene deletion mutants. The wild-type, *FAE* gene deletion mutants and complementation strains were cultured on MSEFA (MS-ethyl ferulate-agar) medium for 3 days. The diameter of the cleared zone generated by the wild-type, *FAE* gene deletion mutants and complementation strains was measured. The FAE activity test was independently carried out three times and each test included three replicates. Bars represent the standard deviation. Different letters represent the statistically significant difference (Tukey's multiple comparison test, $P < 0.05$).

FAEs have been shown to play roles in disease development in plant-pathogenic bacteria (Hassan & Hugouvieux-Cotte-Pattat, 2011). In *Dickeya dadantii*, FAEs have been demonstrated to facilitate soft rot disease (Hassan & Hugouvieux-Cotte-Pattat, 2011). The data of Hassan & Hugouvieux-Cotte-Pattat (2011) showed that *faeD* was clearly expressed in the macerated tissue. The dissociation of the crosslinks in the polysaccharide network, suppression of polysaccharide esterification and synergistic effects with other CWDEs facilitate soft rot disease (Hassan & Hugouvieux-Cotte-Pattat, 2011). During the interaction of *V. mali* with apple tree bark, severe tissue maceration and necrosis are caused, suggesting the action of CWDEs (Ke *et al.*, 2013; Yin *et al.*, 2015). Previously, cytochemical and gene functional studies have revealed that the pectinases of *V. mali* play an important role in colonization and pathogenicity (Ke *et al.*, 2013; Yin *et al.*, 2015). In this study, we demonstrated the pathogenic role of the *FAE* gene family in the *V. mali*–apple tree interaction. Aided by the synergistic effects of FAEs, pectinases and other CWDEs may contribute to the dissociation of crosslinks in the polysaccharide network in apple tree bark. Furthermore, material and nutrition provided by the breakdown of the apple tree bark cell wall promote the development of the apple tree *Valsa* canker.

In plant-pathogenic fungi, redundancy is a CWDE property (Walton, 1994) that impedes the deletion of the genes of interest. The *F. graminearum* genome contains seven *FAE* genes, including three type B, three type C and one type D *FAE* gene. *FAEB1*-, *FAED1*- and double-gene-inactivated mutants do not exhibit a statistically significant reduction in virulence; therefore, *FAEB1* and *FAED1* are not essential for the pathogenicity of *F. graminearum* (Balcerzak *et al.*, 2012). In *Magnaporthe grisea*, *MgFAEA* (*M. grisea FAEA*) shows three hypothetical proteins with a high degree of homology in the genome (Zheng *et al.*, 2009). When one of these genes is lost, the function may be complemented by the other *FAE* genes (Zheng *et al.*, 2009). Similarly, the different FAEs from *Aspergillus niger* have compensatory functions in the degradation of cell wall polysaccharides (de Vries & Visser, 1999).

In *V. mali*, the number of different types of *FAE*s is less than three, which facilitated our work in deleting the *FAE* genes. In this study, we generated single-deletion mutants of all seven of the *FAE* genes. The pathogenicity of single-deletion mutants of *VmFAEA1*, *VmFAEB1* and *VmFAEC1* showed a significant reduction compared with the wild-type strain. To verify whether there is joint action and redundancy of VmFAEs, we generated six double-gene-deletion mutants based on classification and expression pattern. Because only one type A and one type B *FAE* were identified in *V. mali*, we generated the *VmFAEA1B1* double-deletion mutants to verify whether type A and type B FAEs operate either additively or synergistically. Compared with the wild-type strain, deletion of either *VmFAEA1* or *VmFAEB1* resulted in a significant reduction in pathogenicity. Double-deletion mutants of *VmFAEA1B1* showed a greater reduction. These results suggest that *VmFAEA1* and *VmFAEB1* have different substrates, but, alternatively, they may act additively by attacking the same substrate, with the two genes contributing to increase the level of enzyme present. Three type C *FAE* genes were identified in *V. mali*. However, only *VmFAEC1* and *VmFAEC2* were up-regulated during the *V. mali*–apple tree bark interaction. Moreover, *VmFAEC1* and *VmFAEC2* have a close evolutionary relationship. Although the pathogenicity of *VmFAEC1* deletion mutants showed a significant reduction, *VmFAEC2* deletion mutants did not reduce pathogenicity. Further, the pathogenicity of *VmFAEC1C2* double-deletion mutants also showed a greater reduction compared with single-deletion mutants of *VmFAEC1* or *VmFAEC2*. These results suggest the redundancy of type C *FAE*s in *V. mali*. Another type C *FAE* may partly complement the function of the deleted *VmFAEC1* and *VmFAEC2* genes. A similar result has been found previously with regard to secreted exo- and endo-polygalacturonases, which function cooperatively to provide the full virulence of *Fusarium oxysporum* (Bravo Ruiz *et al.*, 2016). Although *VmFAEA1B1* and *VmFAEC1C2* double-deletion mutants showed significant reduction in pathogenicity, double-deletion mutants of *VmFAEB1C1*, *VmFAEB1D1* and *VmFAED1D2* did not show significant reduction. This may be caused by the induced expression of other *VmFAE*s which complement the function of the deleted genes in these *VmFAE* double-deletion mutants, suggesting the redundancy of *FAE* genes in *V. mali*. In another study of polygalacturonase (PG), the expression levels of the other *PG* genes in the *PG* family were obviously affected when both *Vmpg7* and *Vmpg8* were knocked out, especially three genes that were significantly up-regulated (Xu *et al.*, 2016). These data reveal the joint action and redundancy of the *FAE* gene in *V. mali*.

The decrease in the capacity of the *FAE* gene deletion mutants to utilize ethyl ferulate suggests a reduction in the levels of secreted FAEs, which accounts for the decrease in pathogenicity. However, the *VmFAED1* deletion mutant did not show significant reduction in pathogenicity, but reduced overall FAE activity. This is consistent with the results obtained with the *F. graminearum* xylanase FGSG_03624, which contributes significantly to total xylanase activity, but does not contribute to pathogenicity (Sella *et al.*, 2013). *VmFAEC1D1* double-deletion mutants exhibited reduced pathogenicity, but not reduced overall FAE activity, suggesting that the loss of *VmFAEC1* and *VmFAED1* did not affect the degradation of ethyl ferulate in MSEFA medium(MS-ethyl ferulate-agar), but substrates of the apple tree bark cell wall. These results may be explained by the complexity of transcriptional regulation of *FAE* genes. In *F. graminearum*, the expression of *FAEB1* is subject to carbon catabolite repression and is regulated by the xylanolytic transcriptional activator XlnR (Balcerzak *et al.*, 2012). However, when exposed to glucose, xylose and galactose, *FgFAEC1* showed a low level of constitutive expression which is opposite to *FgFAEB1*. Moreover, when cultured in different sugar and aromatic compounds or exposed to maize and wheat hosts, the expression patterns of *FgFAEB2*, *FgFAEB3* and *FgFAED1* were different (Balcerzak *et al.*, 2012). Our results suggest that the regulation of the *FAE* gene family is also complex in *V. mali*. This needs to be explored further.

Our work highlights that the *FAE* genes are required for full pathogenicity of the apple tree canker pathogen *V. mali*. Although *FAE* genes are redundant, our systematic generation of *FAE* gene deletion mutants revealed that different *FAE* genes function cooperatively with regard to pathogenicity in *V. mali*. Pectinases have been demonstrated to be involved in the virulence of *V. mali* (Ke *et al.*, 2013; Xu *et al.*, 2016; Yin *et al.*, 2015). FAE may work in conjunction with pectinases to degrade pectin by the cleavage of ester bonds that crosslink hydroxycinnamic acids and pectins in apple tree bark to facilitate infection and development of *V. mali* in apple tree bark.

EXPERIMENTAL PROCEDURES

Strains and growth conditions

The *V. mali* wild-type strain 03-8 was obtained from the Laboratory of Integrated Management of Plant Diseases at the College of Plant Protection, Northwest A&F University, China, and maintained on potato dextrose agar (PDA) (200 g of potato, 20 g of dextrose, 15 g of agar in 1 L) at 4°C. Cultures of 03-8 and the gene deletion mutants were grown on PDA at 25°C in the dark. Yeast strains, YTK12 and XK1-25, were cultured on yeast peptone dextrose agar (YPDA) (10 g of yeast extract, 20 g of peptone, 20 g of dextrose, 20 g of agar in 1 L) at 30°C. For the generation of the complementation vectors, XK1-25 was cultured on YEPD (3 g of yeast extract, 10 g of peptone, 20 g of dextrose in 1 L), and transformants were cultured on SD-Trp agar medium (6.7 g of yeast nitrogen base without amino acids, 20 g of dextrose, 20 g of agar, 0.74 g of Trp DO Supplement in 1 L), as described previously (Zhou *et al.*, 2011).

Identification of *FAE* genes in *V. mali*

To identify candidate *FAE* genes in the *V. mali* genome, BLAST searches with well-characterized *FAE* genes (*A. niger FAEA*, AF361950; *A. tubingensis FAEA*, Y09331; *N. crassa FAEB*, AJ293029; *Penicillium funiculosum FAEB*, AJ291496; *Talaromyces stipitatus FAEC*, AJ505939; *F. graminearum FAEC*, XM_011324545; *Cellvibrio japonicus xynD*, X58956; *F. graminearum FAED*, XM_011327022) were conducted. The conserved domains of the candidate *FAE* genes were ascertained using the National Center for Biotechnology Information (NCBI) conserved domain database (http://www.ncbi.nlm.nih.gov/Structure/cdd/wrpsb.cgi) (Marchler-Bauer *et al.*, 2015). Primer pairs (Table S1) for the cloning of all the candidate *FAE* genes were synthesized by the Shenggong Company (Shanghai, China). All the genes were amplified using FastPfu DNA polymerase (Transgene, Beijing, China) from a cDNA library of *V. mali* and cloned to T-Vector pMD19 Simple (Takara, Dalian, China). The clones identified by colony PCR were confirmed by sequencing on a 37330xl (Applied Biosystems, Foster City, California, USA).

Sequence alignment and phylogenetic analysis

We performed sequence alignments of the FAEs of *V. mali*, other published FAEs and certain related CWDEs with CLUSTALW using the MEGA7 program with all the parameters set at the default values. The neighbour-joining tree was constructed using MEGA7 with bootstrap replicates set to 1000 (Kumar *et al.*, 2016). The tree was finally visualized using the Interactive Tree Of Life (iTOL) software (http://itol.embl.de/) (Letunic & Bork, 2016). Multiple sequence alignments of the different types of FAEs were performed with CLUSTALW using MEGA7 as described above.

qRT-PCR analysis

Vegetative hyphae were cultured on YEPD (10 g of yeast extract, 20 g of peptone, 20 g of dextrose in 1 L), and the junction of healthy and infected apple bark tissue inoculated with *V. mali* wild-type strain was sampled at 3 dpi. The softened, water-soaked, reddish-brown lesion caused by *V. mali* can be easily identified at this time point. Total RNA was extracted using the Quick RNA Isolation Kit (Huayueyang, Beijing, China), and first-strand cDNA was synthesized using a first-strand cDNA synthesis kit (Promega, Madison, Wisconsin, USA) according to the manufacturer's instructions. The primers used for qRT-PCR analysis are listed in Table S1. A 2 × RealStar Power SYBR Mixture (GenStar, Beijing, China) was used for qRT-PCR. The *V. mali* housekeeping gene *glucose-6-phosphate dehydrogenase* (*G6PDH*) was used as the reference gene (Yin *et al.*, 2013). Relative changes in the transcription level of each gene were calculated using the $2^{-\Delta\Delta Ct}$ method (Livak & Schmittgen, 2001). The transcriptional analyses of the *V. mali FAE* genes were independently repeated three times, and each qRT-PCR analysis contained three technical replicates.

Prediction and verification of the SPs of the VmFAEs

SPs were predicted using SignalP 4.1 (http://www.cbs.dtu.dk/services/SignalP/) (Petersen *et al.*, 2011). To confirm the validity of the predictions, the signal sequence trap method was used (Jacobs *et al.*, 1997). YTK12 and transformants were cultured on CMD-W and YPRAA media, as

described previously (Gu *et al.*, 2011). The coding sequences of the SP of Avr1b and the first 25 amino acids of Mg87 were used as positive and negative controls, respectively (Gu *et al.*, 2011). All the coding sequences of the predicted SPs and the first 25 amino acids of Mg87 were cloned into pSUC2T7M13ORI (pSUC2) using *Eco*RI and *Xho*I, and the fused plasmids were transformed into *Escherichia coli* JM109. All the transformants were tested by PCR and sequenced. The correct plasmids were introduced into the yeast strain YTK12. Transformants were grown on CMD-W and YPRAA media at 30°C for 3 days.

Construction of the gene deletion cassette

The strategy used for the construction of the gene deletion cassettes was derived from the double-joint PCR method (Yu *et al.*, 2004). Figure S3 (see Supporting Information) shows the strategy of gene deletion used in this study. To generate the single *FAE* gene deletion mutants, *VmFAEA1*, *VmFAEC2* and *VmFAEC3* were replaced by *NEO*, and *VmFAEB1*, *VmFAEC1*, *VmFAED1* and *VmFAED2* were replaced by *HPH*. Upstream and downstream fragments of the *V. mali FAE* genes were amplified from 03–8 DNA using two sets of gene-specific primer pairs, 1F/2R and 3F/4R (Table S1). Special 2R and 3F chimeric primers for every gene contained the homologous joints to *HPH* or *NEO*. The *HPH* fragment was amplified from the plasmid pHIG2RHPH2-GFP-GUS using the primers HPH-F and HPH-R, and the *NEO* fragment was amplified from the plasmid pFL2 using the primers NEO-F and NEO-R. The upstream, downstream and *HPH* (or *NEO*) fragments were fused by double-joint PCR (Yu *et al.*, 2004). A nested PCR amplification using the primers CF/CR was necessary. All the gene knock-out cassettes were confirmed by sequencing.

Deletion of *FAE* genes

Protoplast preparation and polyethylene glycol (PEG)-mediated transformation were conducted as described previously (Gao *et al.*, 2011). Regenerated mycelia were mixed with 10 mL of molten bottom agar containing 60 μg/mL hygromycin B (Roche, Mannheim, Germany) or 100 μg/mL geneticin (MP, Solon, Ohio, USA). After 10 h of cultivation at 25°C in the dark, top agar containing 100 μg/mL hygromycin B or 150 μg/mL geneticin was overlaid. After 3–5 days, transformants were picked and inoculated onto PDA containing 100 μg/mL hygromycin B or 150 μg/mL geneticin. Genomic DNA was isolated as described previously (Villalba *et al.*, 2008). PCR detection of the *FAE* gene deletion mutants was carried out by amplification with four primer pairs. The primer pairs 5F/6R and H852/H850 (G852/G850) were used to verify the deletion of *V. mali FAE* and insertion of *HPH* or *NEO*, respectively. The primer pairs 7F/H855R (or G855R) and H856F (or G856F)/VmFAE-8R were used to verify targeted homologous recombination in both upstream and downstream flanks of the gene of interest. For Southern hybridization, 20 μg of genomic DNA was digested by selected restriction endonucleases (Thermo, Waltham, Massachusetts, USA) and subjected to 0.8% agarose gel electrophoresis. DNA was transferred to the positive CHGD nylon transfer membrane (Amersham Biosciences, Piscataway, New Jersey, USA). The synthesis of probes and hybridization were conducted following the Instruction Manual of the DIG High Prime DNA Labeling and Detection Starter Kit II (Roche).

To generate the *FAE* gene double-deletion mutants, the second *FAE* gene was deleted in the single *FAE* deletion mutant utilizing selection on a second antibiotic resistance gene. All the *FAE* double-deletion mutants were also confirmed by PCR and Southern blot analysis.

Generation of complementation strains

For complementation assays, the entire *V. mali FAE* coding sequence and predicted promoter sequence were amplified from genomic DNA using the primer pair CM-F/R (Table S1), and cloned into pFL2 (*VmFAE* genes replaced by *HPH*) or pDL2 (*VmFAE* genes replaced by *NEO*) using the yeast gap repair approach, as described previously (Zhou *et al.*, 2011). Fusion constructs were confirmed by sequencing, and plasmids were transformed into the corresponding deletion mutant via PEG-mediated transformation (Gao *et al.*, 2011). The transformants were confirmed by PCR with the primer pair CM-F/R.

RT-PCR of *VmFAE* in wild-type, FAE gene deletion mutants and complementation mutants

RNA extraction and first-strand cDNA synthesis of cultured mycelium of wild-type, *FAE* gene deletion mutants and complementation mutants were conducted as described previously. Primers used for qRT-PCR were employed to detect *FAE* genes from cDNA of wild-type, *FAE* gene deletion mutants and complementation mutants. The housekeeping gene *G6PDH* was used as a control.

Vegetative growth and pycnidium formation

Mycelium plugs ($d = 5$ mm) from the edge of a growing colony were used to inoculate new PDA plates, which were cultivated at 25°C in the dark for 48 h. Colony shape and colour were observed. Furthermore, the colony diameters were measured. For pycnidia formation, mycelium plugs ($d = 5$ mm) were inoculated onto detached twigs of *M.* × *domestica* Borkh. cv. Fuji as described previously (Wei *et al.*, 2010). The inoculated twigs were cultured at 25°C with a 16-h light and 8-h dark cycle. Pycnidia were counted at 30 dpi. Each experiment was repeated three times and included three replicates. Data were analysed by Tukey's multiple comparison test with SPSS 23.0 (SPSS Inc., Chicago, Illinois, USA) and $P < 0.05$ was considered to be a significant difference.

Infection assays

For the infection assays, annual apple twigs of *M.* × *domestica* Borkh. cv. 'Fuji' with similar growth tendency and thickness from the same test field were collected and inoculated as described previously with a slight modification (Wei *et al.*, 2010). Detached twigs were cut into segments of 30 cm in length and washed with tap water. For surface sterilization, the twigs were immersed in sterilized distilled water with 0.6% (v/v) sodium hypochlorite for 10 min. The twigs were washed with sterilized distilled water three times and sealed with paraffin at both ends. Then, three evenly distributed wounds were made with a cork borer (diameter, 5 mm) in the upper, middle and lower regions of the twig segments. Mycelium plugs ($d = 5$ mm) from the edge of a growing colony on SYA medium (5 g of sucrose, 0.5 g of yeast extract, 15 g of agar in 1 L) were inoculated onto wounds. Each group of infection assays included three treated twigs. The wild-type strain, the *FAE* gene deletion mutant and the complementation strain (or another *FAE* gene deletion mutant) were rotationally

inoculated to the upper, middle and lower wounds in the three different apple twigs. SYA medium plugs ($d = 5$ mm) were used as control. The inoculated twigs were placed in trays, and the trays were covered with parafilm to retain humidity. Then, the inoculated twigs were cultured at 25°C in the dark. The maximum lesion length was measured at 5 dpi. The infection assays were independently repeated three times with three twigs per experiment. The pathogenicity data were analysed using Fisher's least-significant difference (LSD) test with SPSS 23.0 (SPSS Inc.). $P < 0.05$ was considered to be a significant difference.

FAE activity assays

To detect FAE activity, MS medium (PhytoTechnology Laboratories, Shawnee Mission, Kans, USA) containing 0.2% (w/v) ethyl ferulate (Sigma, St. Louis, Missouri, USA), which acted as the sole carbon source, was used to culture 03–8 and the *FAE* gene deletion mutants following the described method (Pinto, 2015) with a slight modification. Mycelium plugs ($d = 5$ mm) from the edge of a colony growing on SYA medium were used to inoculate MSEFA and cultured at 25°C in the dark for 3 days. Afterwards, the diameter of the cleared areas was measured. Experiments were repeated three times and included three replicates. Data were analysed by Tukey's multiple comparison test with SPSS 23.0 (SPSS Inc.). $P < 0.05$ was considered to be a significant difference.

ACKNOWLEDGEMENTS

We thank Professor Ralf T. Voegele at Universität Hohenheim for careful reading of the manuscript. We thank Professor Fengming Song at Zhejiang University for providing the pHIG2RHPH2-GFP-GUS plasmid. We also thank Professor Jin-Rong Xu at Northwest A&F University for providing the pFL2 and pDL2 plasmids. This work was supported by the National Natural Science Foundation of China (31301606).

CONFLICTS OF INTEREST

The authors declare that no competing interests exist.

REFERENCES

Adams, G.C., Roux, J. and Wingfield, M.J. (2006) *Cytospora* species (*Ascomycota*, *Diaporthales*, *Valsaceae*): introduced and native pathogens of trees in South Africa. *Australas. Plant Pathol.* **35**, 521.

Balcerzak, M., Harris, L.J., Subramaniam, R. and Ouellet, T. (2012) The feruloyl esterase gene family of *Fusarium graminearum* is differentially regulated by aromatic compounds and hosts. *Fungal Biol.* **116**, 478–488.

Benoit, I., Navarro, D., Marnet, N., Rakotomanomana, N., Lesage-Meessen, L., Sigoillot, J., Asther, M. and Asther, M. (2006) Feruloyl esterases as a tool for the release of phenolic compounds from agro-industrial by-products. *Carbohydr. Res.* **341**, 1820–1827.

Biggs, A.R. (1989) Integrated approach to controlling Leucostoma canker of peach in Ontario. *Plant Dis.* **73**, 869–874.

Borneman, W.S., Ljungdahl, L.G., Hartley, R.D. and Akin, D.E. (1992) Purification and partial characterization of two feruloyl esterases from the anaerobic fungus *Neocallimastix* strain MC-2. *Appl. Environ. Microbiol.* **58**, 3762–3766.

Bravo Ruiz, G., Di Pietro, A. and Roncero, M.I.G. (2016) Combined action of the major secreted exo- and endopolygalacturonases is required for full virulence of *Fusarium oxysporum*. *Mol. Plant Pathol.* **17**, 339–353.

Cosgrove, D.J. (2005) Growth of the plant cell wall. *Nat. Rev. Mol. Cell. Biol.* **6**, 850–861.

Crepin, V.F., Faulds, C.B. and Connerton, I.F. (2004) Functional classification of the microbial feruloyl esterases. *Appl. Microbiol. Biotechnol.* **63**, 647–652.

Dixon, R.A. (2013) Microbiology break down the walls. *Nature*, **493**, 36–37.

Faulds, C.B. and Williamson, G. (1994) Purification and characterization of a ferulic acid esterase (FAE-III) from *Aspergillus niger* specificity for the phenolic moiety and binding to microcrystalline cellulose. *Microbiology*, **140**, 779–787.

Feng, J. (2005) A secreted lipase encoded by *LIP1* is necessary for efficient use of saturated triglyceride lipids in *Fusarium graminearum*. *Microbiology*, **151**, 3911–3921.

Fu, H., Feng, J., Aboukhaddour, R., Cao, T., Hwang, S.F. and Strelkov, S.E. (2013) An exo-1,3-beta-glucanase GLU1 contributes to the virulence of the wheat tan spot pathogen *Pyrenophora tritici-repentis*. *Fungal Biol.* **117**, 673–681.

Gao, J., Li, Y., Ke, X., Kang, Z. and Huang, L. (2011) Development of genetic transformation system of *Valsa mali* of apple mediated by PEG. *Acta Microbiol. Sin.* **51**, 1194–1199.

Gopalan, N., Rodríguez-Duran, L.V., Saucedo-Castaneda, G. and Nampoothiri, K.M. (2015) Review on technological and scientific aspects of feruloyl esterases: a versatile enzyme for biorefining of biomass. *Bioresour. Technol.* **193**, 534–544.

Gu, B., Kale, S.D., Wang, Q., Wang, D., Pan, Q., Cao, H., Meng, Y., Kang, Z., Tyler, B.M. and Shan, W. (2011) Rust secreted protein Ps87 is conserved in diverse fungal pathogens and contains a RXLR-like motif sufficient for translocation into plant cells. *PLoS One*, **6**, e27217.

Guerriero, G., Hausman, J., Strauss, J., Ertan, H. and Siddiqui, K.S. (2015) Destructuring plant biomass: focus on fungal and extremophilic cell wall hydrolases. *Plant Sci.* **234**, 180–193.

Hassan, S. and Hugouvieux-Cotte-Pattat, N. (2011) Identification of two feruloyl esterases in *Dickeya dadantii* 3937 and induction of the major feruloyl esterase and of pectate lyases by ferulic acid. *J Bacteriol.* **193**, 963–970.

Hermoso, J.A., Sanz-Aparicio, J., Molina, R., Juge, N., González, R. and Faulds, C.B. (2004) The crystal structure of feruloyl esterase A from *Aspergillus niger* suggests evolutive functional convergence in feruloyl esterase family. *J Mol. Biol.* **338**, 495–506.

Hu, Y., Dai, Q.Q., Liu, Y.Y., Yang, Z., Song, N., Gao, X.N., Voegele, R.T., Kang, Z.S. and Huang, L.L. (2014) *Agrobacterium tumefaciens*-mediated transformation of the causative agent of Valsa canker of apple tree *Valsa mali* var. *mali*. *Curr. Microbiol.* **68**, 769–776.

Huang, D.X., Yang, H.U., Sun, G.C., Gao, X.N., Yin, Z.Y. and Huang, L.L. (2014) Phenotype and pathogenicity of *Valsa mali* T-DNA insertion mutants. J. Northwest A&F University, **42**, 113–121.

Ishii, T. (1997) Structure and functions of feruloylated polysaccharides. *Plant Sci.* **127**, 111–127.

Jacobs, K.A., Collins-Racie, L.A., Colbert, M., Duckett, M.K., Golden-Fleet, M., Kelleher, K., Kriz, R., LaVallie, E.R., Merberg, D., Spaulding, V., Stover, J., Williamson, M.J. and McCoy, J.M. (1997) A genetic selection for isolating cDNAs encoding secreted proteins. *Gene*, **198**, 289–296.

Ke, X.W., Huang, L.L., Han, Q.M., Gao, X.N. and Kang, Z.S. (2013) Histological and cytological investigations of the infection and colonization of apple bark by *Valsa mali* var. *mali*. *Australas. Plant Pathol.* **42**, 85–93.

Ke, X.W., Yin, Z.Y., Song, N., Dai, Q.Q., Voegele, R.T., Liu, Y.Y., Wang, H.Y., Gao, X.N., Kang, Z.S. and Huang, L.L. (2014) Transcriptome profiling to identify genes involved in pathogenicity of *Valsa mali* on apple tree. *Fungal Genet. Biol.* **68**, 31–38.

Kepley, J.B. and Jacobi, W.R. (2000) Pathogenicity of *Cytospora* fungi on six hardwood species. *J Arboric.* **26**, 326–333.

Kikot, G.E., Hours, R.A. and Alconada, T.M. (2009) Contribution of cell wall degrading enzymes to pathogenesis of *Fusarium graminearum*: a review. *J Basic Microbiol.* **49**, 231–241.

Kubicek, C.P., Starr, T.L. and Glass, N.L. (2014) Plant cell wall-degrading enzymes and their secretion in plant-pathogenic fungi. *Annu. Rev. Phytopathol.* **52**, 427–451.

Kumar, S., Stecher, G. and Tamura, K. (2016) MEGA7: molecular evolutionary genetics analysis version 7.0 for bigger datasets. *Mol. Biol. Evol.* **33**, 1870–1874.

Letunic, I. and Bork, P. (2016) Interactive tree of life (iTOL) v3: an online tool for the display and annotation of phylogenetic and other trees. *Nucleic Acids Res.* **44**, W242–W245.

Livak, K.J. and Schmittgen, T.D. (2001) Analysis of relative gene expression data using real-time quantitative PCR and the $2^{-\Delta\Delta CT}$ method. *Methods*, **25**, 402–408.

Mackenzie, C.R., Bilous, D., Schneider, H. and Johnson, K.G. (1987) Induction of cellulolytic and xylanolytic enzyme systems in *Streptomyces* spp. *Appl. Environ. Microbiol.* **53**, 2835–2839.

Marchler-Bauer, A., Derbyshire, M.K., Gonzales, N.R., Lu, S., Chitsaz, F., Geer, L.Y., Geer, R.C., He, J., Gwadz, M., Hurwitz, D. I., Lanczycki, C.J., Lu, F., Marchler, G.H., Song, J.S., Thanki, N., Wang, Z., Yamashita, R.A., Zhang, D.,

Zheng, C. and Bryant, S.H. (2015) CDD: NCBI's conserved domain database. *Nucleic Acids Res.* **43**, D222–D226.
Petersen, T.N., Brunak, S., von Heijne, G. and Nielsen, H. (2011) SignalP 4.0: discriminating signal peptides from transmembrane regions. *Nat. Methods*, **8**, 785–786.
Pinto, C. (2015) Feruloyl esterase: a principal biodegradative enzyme. In: *Bioprospects of Coastal Eubacteria* (Borkar, S., ed), pp. 209–224. Switzerland: Springer International Publishing.
Sella, L., Gazzetti, K., Faoro, F., Odorizzi, S., D'Ovidio, R., Schäfer, W. and Favaron, F. (2013) A *Fusarium graminearum* xylanase expressed during wheat infection is a necrotizing factor but is not essential for virulence. *Plant Physiol. Biochem.* **64**, 1–10.
Topakas, E., Vafiadi, C. and Christakopoulos, P. (2007) Microbial production, characterization and applications of feruloyl esterases. *Process Biochem.* **42**, 497–509.
Van Vu, B., Itoh, K., Nguyen, Q.B., Tosa, Y. and Nakayashiki, H. (2012) Cellulases belonging to glycoside hydrolase families 6 and 7 contribute to the virulence of *Magnaporthe oryzae*. *Mol. Plant–Microbe Interact.* **25**, 1135–1141.
Vasilyeva, L. and Kim, W. (2000) *Valsa mali* Miyabe et Yamada, the causal fungus of apple tree canker in east Asia. *Mycobiology*, **28**, 153–157.
Villalba, F., Collemare, J., Landraud, P., Lambou, K., Brozek, V., Cirer, B., Morin, D., Bruel, C., Beffa, R. and Lebrun, M. (2008) Improved gene targeting in *Magnaporthe grisea* by inactivation of MgKU80 required for non-homologous end joining. *Fungal Genet. Biol.* **45**, 68–75.
de Vries, R.P. and Visser, J. (1999) Regulation of the feruloyl esterase (*faeA*) gene from *Aspergillus niger*. *Appl. Environ. Microbiol.* **65**, 5500–5503.
Walton, J.D. (1994) Deconstructing the cell wall. *Plant Physiol.* **104**, 1113–1118.
Wang, X.L., Zang, R., Yin, Z.Y., Kang, Z.S. and Huang, L.L. (2014) Delimiting cryptic pathogen species causing apple Valsa canker with multilocus data. *Ecol. Evol.* **4**, 1369–1380.
Wei, J.L., Huang, L.L., Gao, Z.P., Ke, X.W. and Kang, Z.S. (2010) Laboratory evaluation methods of apple Valsa canker disease caused by *Valsa ceratosperma* sensu Kobayashi. *Acta Phytopathol. Sin.* **40**, 14–20.
Wong, D.W. (2006) Feruloyl esterase: a key enzyme in biomass degradation. *Appl. Biochem. Biotechnol.* **133**, 87–112.
Wong, D.W., Chan, V.J., Batt, S.B., Sarath, G. and Liao, H. (2011) Engineering *Saccharomyces cerevisiae* to produce feruloyl esterase for the release of ferulic acid from switchgrass. *J Ind. Microbiol. Biotechnol.* **38**, 1961–1967.
Xu, C.J., Wu, Y.X., Dai, Q.Q., Li, Z.P., Gao, X.N. and Huang, L.L. (2016) Function of polygalacturonase genes *Vmpg7* and *Vmpg8* of *Valsa mali*. *Sci. Agric. Sin.* **8**, 1489–1498.
Yin, Z.Y., Ke, X.W., Huang, D.X., Gao, X.N., Voegele, R.T., Kang, Z.S. and Huang, L.L. (2013) Validation of reference genes for gene expression analysis in *Valsa mali* var. *mali* using real-time quantitative PCR. *World J Microbiol. Biotechnol.* **29**, 1563–1571.
Yin, Z.Y., Liu, H.Q., Li, Z.P., Ke, X.W., Dou, D.L., Gao, X.N., Song, N., Dai, Q.Q., Wu, Y.X., Xu, J.R., Kang, Z.S. and Huang, L.L. (2015) Genome sequence of Valsa canker pathogens uncovers a potential adaptation of colonization of woody bark. *New Phytol.* **208**, 1202–1216.
Yu, J., Hamari, Z., Han, K., Seo, J., Reyes-Domínguez, Y. and Scazzocchio, C. (2004) Double-joint PCR: a PCR-based molecular tool for gene manipulations in filamentous fungi. *Fungal Genet. Biol.* **41**, 973–981.
Zheng, X., Zhou, J., Lin, C., Lin, X., Lan, L., Wang, Z. and Lu, G.D. (2009) Secretion property and gene expression pattern of a putative feruloyl esterase in *Magnaporthe grisea*. In: *Advances in Genetics, Genomics and Control of Rice Blast Disease* (Wang, G.-L. and Valent, B., eds), pp. 41–50. Dordrecht: Springer.
Zhou, X., Li, G. and Xu, J. (2011) Efficient approaches for generating GFP fusion and epitope-tagging constructs in filamentous fungi. *Methods Mol. Biol.* **722**, 199–212.

SUPPORTING INFORMATION

Additional Supporting Information may be found in the online version of this article at the publisher's website:

Fig. S1 Conserved domains of the candidate *ferulic acid esterase* (*FAE*) genes.

Fig. S2 Prediction of the signal peptides of the *Valsa mali* ferulic acid esterases (VmFAEs) by SignalP 4.1.

Fig. S3 Diagram of strategy of gene deletion used in this study.

Fig. S4 Polymerase chain reaction (PCR) detection of the *Valsa mali ferulic acid esterase* (*VmFAE*) deletion mutants. Four primer pairs were used to detect the mutants. Four lines (from left to right) in the agarose gel for each mutant were loaded DNA products amplified by the primer pairs 5F/6R (detection of the target gene), H852/H850 (G852/G850) (detection of the resistance gene), 7F/H855R (G855R) (detection of the upstream homologous recombination) and H856F (G856F)/8R (detection of the downstream homologous recombination), respectively. In (E), (G) and (M), the wild-type strain 03-8 and pFL2 plasmid were used as positive control for detection of the target gene and resistance gene, respectively; sterile double-distilled H_2O (ddH_2O) was used as a negative control.

Fig. S5 Construction of the *ferulic acid esterase* (*FAE*) gene replacement cassettes and Southern blot analysis of the *FAE* deletion mutants of *Valsa mali*. (A) Deletion of *VmFAEA1*; (B) deletion of *VmFAEB1* and double deletion of *VmFAEB1* based on A1-52; (C) deletion of *VmFAEC1*; (D) deletion of *VmFAEC2*; (E) deletion of *VmFAED1*; (F) double deletion of *VmFAEC1* based on B1-5; (G) double deletion of *VmFAEC2* based on C1-71; (H) double deletion of *VmFAED1* based on B1-5 and C1-71.

Fig. S6 Polymerase chain reaction (PCR) detection of complementation strains. VmFAE-CM-F/R were used to detect the complementary fragments from the genomic DNA of complementation strains.

Fig. S7 Reverse transcription-polymerase chain reaction (RT-PCR) detection of *Valsa mali ferulic acid esterases* (*VmFAEs*) from wild-type, *VmFAE* gene deletion mutants and complementation strains. The housekeeping gene *glucose-6-phosphate dehydrogenase* (*G6PDH*) was used as control.

Fig. S8 Pycnidia formation by wild-type and *ferulic acid esterase* (*FAE*) gene deletion mutants. Photographs were taken at 30 days post-inoculation (dpi). (A) Pycnidia formation on apple twigs by wild-type and *FAE* gene deletion mutants. The black points on the apple twigs are the pycnidia of *Valsa mali*. (B) Number of pycnidia per square centimetre on apple twigs. Mean and standard deviation were calculated from three independent experiments with three replicates per experiment. Bars represent the standard deviation.

Fig. S9 Pathogenicity measurement of additional *Valsa mali ferulic acid esterase* (*VmFAE*) deletion mutants. Wild-type, *FAE* gene deletion mutants and complementation strains were inoculated onto twigs of *Malus* × *domestica* Borkh. cv. Fuji. SYA (sucrose–yeast extract–agar) medium plugs ($d = 5$ mm) were used as control (CK). Photographs were taken at 5 days post-inoculation (dpi). Each experiment was repeated independently three times, and each experiment included three replicates. Bars represent the standard deviation.

Table S1 Polymerase chain reaction primers used in this study.